The R345W mutation in *EFEMP1* is pathogenic and causes AMD-like deposits in mice

Li Fu[1], Donita Garland[1], Zhenglin Yang[2,3], Dhananjay Shukla[4], Anand Rajendran[4], Erik Pearson[2,3], Edwin M. Stone[5], Kang Zhang[2,3] and Eric A. Pierce[1,*]

[1]F.M. Kirby Center for Molecular Ophthalmology, University of Pennsylvania School of Medicine, Philadelphia, PA, USA, [2]Department of Ophthalmology and Visual Sciences, [3]Program in Human Molecular Biology and Genetics, Eccles Institute of Human Genetics, University of Utah Health Sciences Center, Salt Lake City, UT, USA, [4]Aravind Eye Hospital and Postgraduate Institute of Ophthalmology, Madurai, Tamil Nadu, India and [5]Howard Hughes Medical Institute and Department of Ophthalmology, University of Iowa Carver College of Medicine, Iowa City, IA, USA

Age-related macular degeneration (AMD) is the most common cause of vision loss in developed countries. A defining characteristic of this disorder is the accumulation of material between Bruch's membrane and the retinal pigment epithelium (RPE), first as microscopic basal deposits and later as clinically evident drusen. The pathogenesis of these deposits remains to be defined. Biochemical and genetic studies have suggested that inflammation and complement activation may play roles in AMD. Several lines of evidence also suggest that alterations to the extracellular matrix (ECM) of the RPE and choroid contribute to the development of AMD. The inherited macular degeneration Doyne honeycomb retinal dystrophy/Malattia Leventinese is thought to be caused by an R345W mutation in the *EFEMP1* gene (also called fibulin-3). The pathogenicity of this mutation has been questioned because all individuals identified to date with the R345W mutation have shared a common haplotype. We investigated the pathogenicity of this mutation in families with early-onset macular degeneration and by generating *Efemp1*-R345W knockin mice. Genetic studies show that one of the identified families with the R345W mutation has a novel haplotype. The mutant *Efemp1*-R345W mice develop deposits of material between Bruch's membrane and the RPE, which resemble basal deposits in patients with AMD. These basal deposits contain Efemp1 and Timp3, an Efemp1 interacting protein. Evidence of complement activation was detected in the RPE and Bruch's membrane of the mutant mice. These results confirm that the R345W mutation in *EFEMP1* is pathogenic. Further, they suggest that alterations in the ECM may stimulate complement activation, demonstrating a potential connection between these two etiologic factors in macular degeneration.

INTRODUCTION

Age-related macular degeneration (AMD) is the most common cause of severe and irreversible vision loss in developed countries (1). The most characteristic clinical finding in the maculae of patients with AMD is drusen. Drusen are extracellular deposits of protein and lipid, which accumulate between the retinal pigment epithelium (RPE) and Bruch's membrane in the macula (2). The geographic atrophy and choroidal neovascularization

(CNV), which are major causes of vision loss in AMD, are thought to be a consequence of drusen or the processes leading to drusen formation. Anti-angiogenic therapies have recently been shown to be successful for treating CNV (3). There are, however, only limited treatments available to prevent the progression of AMD and no therapies for preventing vision loss from the more common atrophic form of the disease (4).

On the basis of the observations from patient samples, it is thought that the precursors of drusen are basal deposits. These

*To whom correspondence should be addressed at: F.M. Kirby Center for Molecular Ophthalmology, University of Pennsylvania School of Medicine, 305 Stellar Chance Labs, 422 Curie Boulevard, Philadelphia, PA 19104, USA. Tel: +1 2155733919; Fax: +1 2155738030; Email: epierce@mail.med.upenn.edu

are microscopic accumulations of material between Bruch's membrane and the RPE (5). At present, it is not known why basal deposits form and how they become drusen. Some insight into the pathogenesis of AMD has been gained from studying the genetics of inherited macular degenerations and more recently from genetic association studies of the age-related condition. Mutations in genes that encode proteins involved in lipid metabolism (*ELOVL4* and *ABCA4*) and extracellular matrix (ECM) integrity (*TIMP3*, *EFEMP1* and *C1QTNF5*) have been found to cause inherited macular degenerations (6–10).

Genetic association studies have recently demonstrated that sequence alterations in the genes for complement factor H (*CFH*), toll-like receptor 4 (*TLR4*) and HtrA serine peptidase 1 (*HTRA1*) are associated with an increased risk of developing AMD (11–19). The associations of *CFH* and *TLR4* with AMD are consistent with earlier work, suggesting that alterations in inflammatory and immune processes contribute to the pathogenesis of AMD (20). A role of oxidative stress AMD pathogenesis is supported by population-based studies, which demonstrated that antioxidants can reduce the progression of AMD and studies implicating iron overload as a causative factor in AMD (4,21). All these findings are consistent with the hypothesis that AMD is a multi-factorial or common complex disorder.

Several lines of evidence indicate that alterations in the integrity of the ECM are important contributors to the pathogenesis of macular degeneration. The HtrA serine peptidase 1 is thought to regulate degradation of ECM components (22). The disorder Doyne honeycomb retinal dystrophy/Malattia Leventinese (DHRD/ML) is thought to be caused by an R345W mutation in the *EFEMP1* gene (EGF-containing fibrillin-like ECM protein 1; also called fibulin-3) (9). The R345W mutation in *EFEMP1* was first identified in 161 individuals from 39 families with DHRD/ML. The mutation was not present in 477 control individuals or in 494 patients with AMD (9). Of note, all affected individuals described in this initial report shared a common disease haplotype, suggesting that the R345W mutation arose once in a common ancestor, but this also raised the possibility that the R345W variant was in linkage disequilibrium with the true disease-causing gene/mutation located nearby.

The EFEMP1 protein is a member of the fibulin family of ECM proteins. The six fibulin family members share an elongated structure and tandem arrays of epidermal growth factor-like domains and are widely expressed in the basement membranes of epithelia and blood vessels (23). Genetic studies have further implicated other fibulins in the pathogenesis of AMD. A study of 402 unrelated patients with the clinical diagnosis of AMD showed that 1.7% of these patients exhibited amino acid altering sequence variations in fibulin-5, a finding not observed in 429 control patients (24). Additionally, other study participants affected with AMD demonstrated variations in highly conserved residues of other fibulin genes.

Some fibulin proteins play essential roles in the assembly of elastin fibers, but the function of EFEMP1 is not known at present (25–28). *EFEMP1* mRNA is expressed most abundantly in the retina and lung (9,29). EFEMP1 has been shown to interact with TIMP3, and both proteins co-localize to the basal deposits of patients with DHRD/ML (30,31).

The mechanisms by which the identified mutations in *EFEMP1* and other ECM components lead to the clinical manifestations of macular degeneration are not understood. We have pursued two avenues of study to investigate the role of EFEMP1 in macular degeneration. First, we genetically characterized two families with DHRD/ML, including one new family from India. Secondly, we generated *Efemp1*-R345W point mutation knockin mice. Our results confirm the pathogenic role of the R345W mutation in *EFEMP1* and highlight the importance of ECM components in the earliest stages of macular degeneration.

RESULTS

Clinical studies

Two families with the clinical phenotype of DHRD/ML were examined. Of the 17 subjects of family A examined, 10 were affected and 7 were unaffected (Fig. 1A). Family A was a branch of one of the families described in the original study by EMS in 1999 (9). Ages of examined individuals ranged from 19 to 76 years. Visual acuities ranged from 20/20 in asymptomatic young patients to count-fingers in older affected individuals. Fundus examination revealed near-confluent drusen in a radial pattern (Fig. 2).

Family B is from India and exhibits consanguinity (Fig. 1B). The mother, father and two sons were examined. Ages ranged from 12 to 48 years and visual acuity from 20/20 to 20/800. The two sons exhibited significantly more severe phenotypes than either parent, particularly the older son whose retina demonstrated drusen extending beyond the posterior pole with associated retinal degeneration (Fig. 2). Sequence analysis revealed that the two children were homozygous for the R345W mutation (Fig. 1C).

Genotype analysis of these two families performed with two microsatellite markers flanking the *EFEMP1* gene and three SNPs within *EFEMP1* gene revealed different haplotypes. Family A's haplotype is identical to all previously reported haplotypes associated with the R345W mutation, whereas the disease haplotype in family B is distinctly different, suggesting that this mutation arose independently (Fig. 1).

Generation of *Efemp1*-R345W mice

The R345W mutation was introduced into the *Efemp1* gene of mouse embryonic stem (ES) cells using gene-targeting techniques (Fig. 3) (32,33). Two ES cell clones with the *Efemp1*-R345W-Neo allele were injected into blastocysts to generate chimeric mice. Mice with the *Efemp1*-R345W (ki) allele were generated by crossing F1 Neo mice with universal Cre-deleter mice (34). Southern blotting and sequence analyses showed transmission of the ki allele to progeny (Fig. 3). Intercrosses of heterozygous $Efemp1^{+/R345W}$ mice generated the expected number of wild-type, $Efemp1^{+/R345W}$ and $Efemp1^{R345W/R345W}$ mice. The homozygous $Efemp1^{R345W/R345W}$ mice are fertile, have normal weights and a normal lifespan and do not demonstrate evidence of systemic disease.

The mRNA from the mutant *Efemp1*-R345W allele was expressed at levels equal to those observed from the wild-type
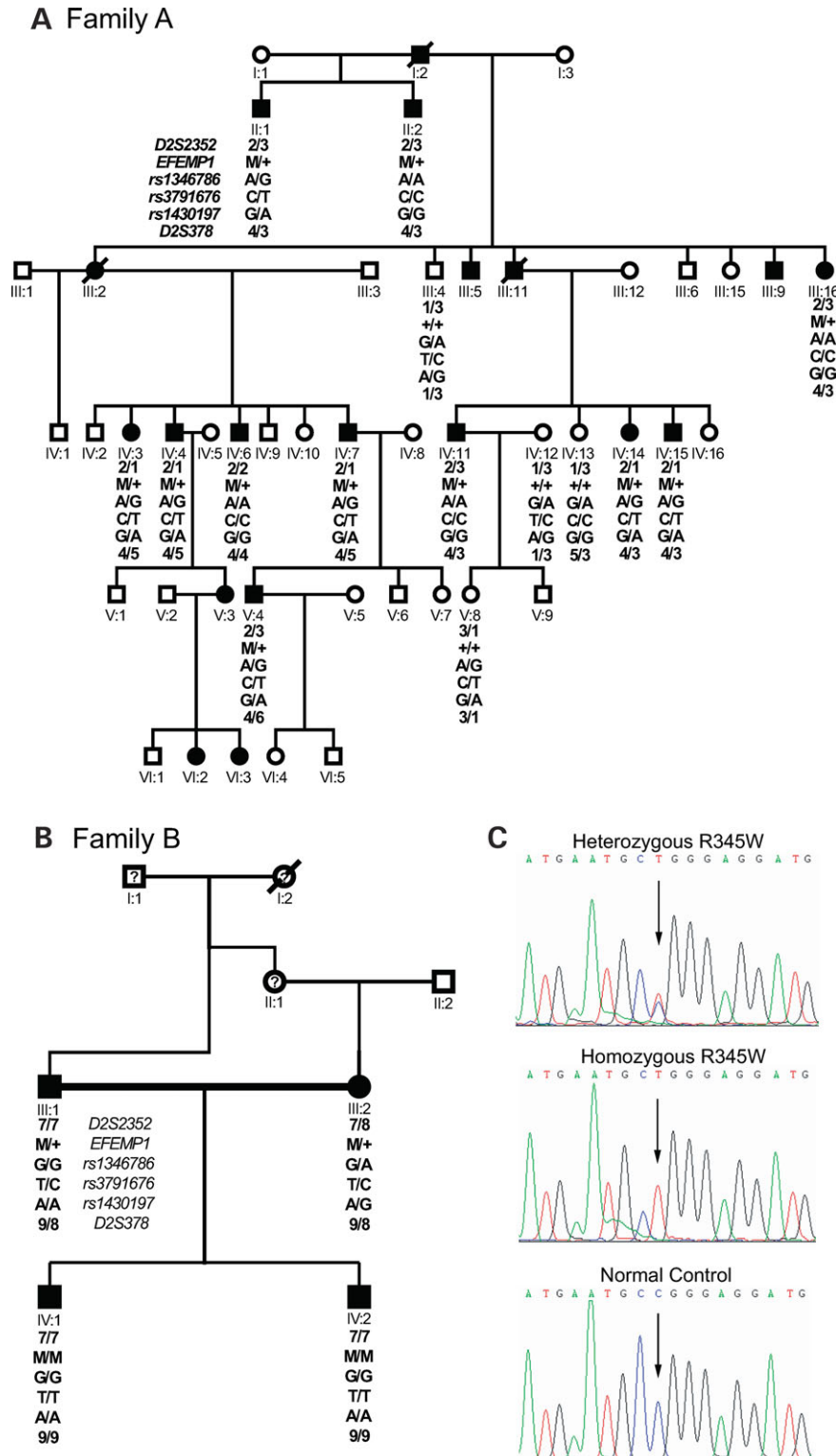
Figure 1. Pedigrees of two families affected by DHRD/ML. (**A**) Pedigree of a branch of a family described by Stone *et al.* (9) showing an autosomal-dominant pattern of inheritance. (**B**) Pedigree of a family from India also showing an autosomal-dominant pattern of inheritance. Haplotype data for two microsatellite markers flanking the *EFEMP1* gene and three SNPs within *EFEMP1* gene are shown for 14 individuals of family A and four individuals of family B. Family B exhibits a novel disease haplotype suggesting an independent mutation. 2-M-A-C-G-4 is the disease haplotype in family A and 7-M-G-T-A-9 is the disease haplotype in family B. Family members are identified by generation and individual numbers. Squares, males; circles, females; slashed symbols, deceased; solid symbols, affected; open symbols, unaffected; +, normal *EFEMP1* gene; M, *EFEMP1* gene with R345W mutation. (**C**) DNA sequence traces of a segment of *EFEMP1* from representative members of family B showing a C-to-T heterozygous missense mutation (top), a homozygous C-to-T mutation (middle) and a normal control (bottom). This C-to-T mutation results in an arginine-to-histidine change at codon 345 in a highly conserved region of *EFEMP1*. The color-coded tracings correspond to the four DNA bases: adenine (green), cytosine (blue), guanine (black) and thymine (red).
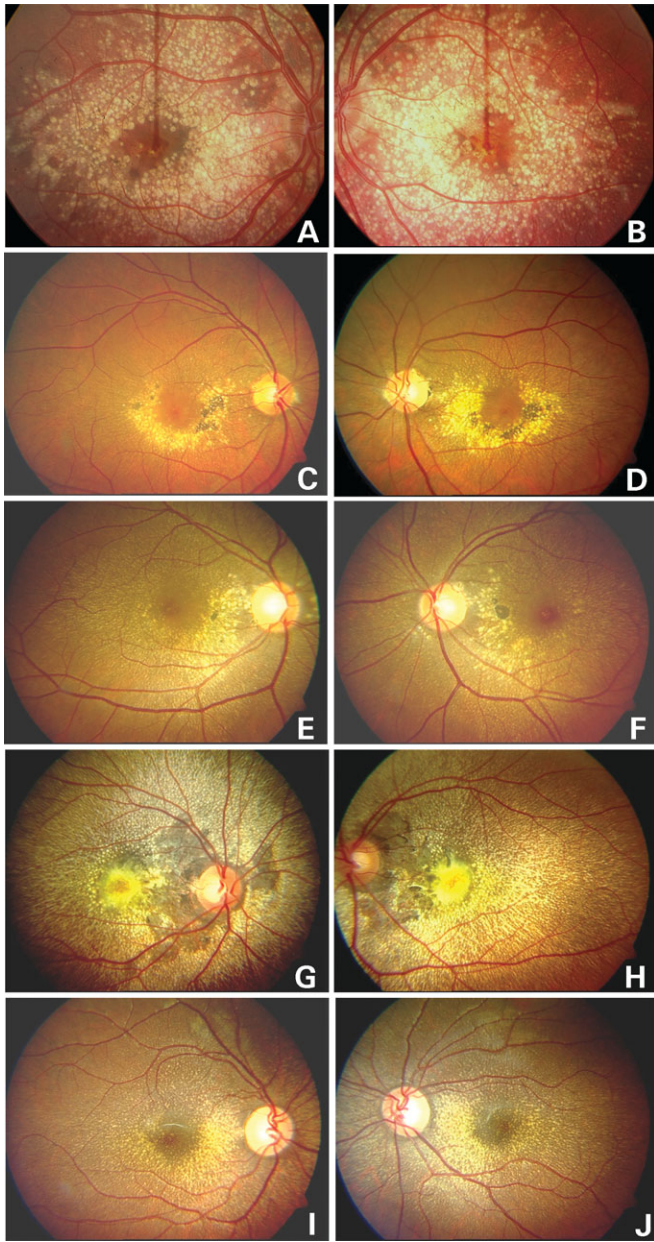
Figure 2. Fundus photographs of patients with DHRD/ML. Photos of one affected individual from family A [VI:3 (**A**) and (**B**)] and four affected individuals from family B [III:1 (**C**) and (**D**); III:2 (**E** and (**F**); IV:1 (**G** and (**H**) and IV:2 (**I**) and (**J**)]. All photos show drusen and associated retinal degeneration in a radial pattern. (G–J) are of young individuals homozygous for the R345W mutation in *EFEMP1*. Both children exhibit phenotypes more severe than either of their parents, seen in (C–F).

allele (Fig. 4A). Similarly, Efemp1 protein levels were similar in the eyes of wild-type, *Efemp1*$^{+/R345W}$ and *Efemp1*$^{R345W/R345W}$ mice (Fig. 4B).

Phenotype of the *Efemp1*-R345W mice

A series of experiments were performed to define the ocular phenotype of the *Efemp1*-R345W mice. Mice were evaluated at 2, 6, 12 and 18 months of age. Fundoscopic examination of the retinas of *Efemp1*$^{+/R345W}$ and *Efemp1*$^{R345W/R345W}$ mice did not reveal abnormalities at any of the ages evaluated (Supplementary Material, Fig. S1). Similarly, fluorescein angiography of the *Efemp1*$^{R345W/R345W}$ mice at 12 months of age was normal (Supplementary Material, Fig. S1). Electroretinogram (ERG) analysis of the homozygous *Efemp1*$^{R345W/R345W}$ and control mice at 12 months of age showed normal rod and cone function (data not shown).

Histological evaluation shows that the neural retinas of *Efemp1*-R345W mutant mice appear essentially normal from 6 to 18 months of age (Fig. 5). At the 12- and 18-month timepoints, however, it was noted that small clear spaces developed in the RPE from *Efemp1*$^{R345W/R345W}$ mice (Fig. 5). Electron microscopy confirms that vacuoles develop in the RPE of the homozygous mutant mice as early as 6 months of age and are extensive by 12 months of age (Fig. 6; Supplementary Material, Fig. S2). Staining of sections of retinas from homozygous *Efemp1*$^{R345W/R345W}$ mice with oil red O and filipin did not detect the lipid or cholesterol in the RPE vacuoles (data not shown).

Electron microscopic analyses also detected abnormalities of Bruch's membrane in *Efemp1*$^{R345W/R345W}$ mice, beginning with deposits of wide-spaced collagen within Bruch's membrane at 2 months of age (Fig. 6). At 6 months, small deposits were detected between Bruch's membrane and the RPE. These deposits were more notable by 12 months of age and disrupted the normal organization of the basolateral infoldings of the RPE (Fig. 6). The deposits consist of amorphous electron dense material and appear to arise from Bruch's membrane. Over time the deposits continued to increase in size and, by 18 months, were several microns thick (Fig. 6, Supplementary Material, Fig. S2). Membranous debris was also noted in some of the deposits at 18 months of age (Supplementary Material, Fig. S2). Heterozygous *Efemp1*$^{+/R345W}$ mice also develop deposits by 18 months, although these are smaller in size than those observed in the *Efemp1*$^{R345W/R345W}$ mice (data not shown).

To assess the extent of deposit and RPE vacuole distribution in the retinas of *Efemp1*-R345W mice, we divided each section of retina (nerve to ora) into 20 segments and scored each segment for the presence of deposits and/or vacuoles using electron microscopy. The RPE vacuoles and basal deposits were detected in 80 and 95% of the segments of *Efemp1*$^{R345W/R345W}$ mice by 12 months of age (Table 1). Heterozygous *Efemp1*$^{+/R345W}$ mice developed vacuoles by 6 months of age, but deposits were not detected at 12 months. No deposits were observed in wild-type *Efemp1*$^{+/+}$ mice. A lower percentage (25%) of the wild-type mice developed vacuoles by 12 months of age. This has been observed previously in aging mice and rats (35,36).

Composition of basal deposits in *Efemp1*-R345W mice

We performed immunofluorescence microscopy to ask whether the basal deposits observed in the *Efemp1*$^{R345W/R345W}$ mice contained Efemp1 protein. The Efemp1 signal was clearly increased in Bruch's membrane of 12-month-old *Efemp1*$^{R345W/R345W}$ mice when compared with wild-type littermate controls (Fig. 7). As EFEMP1 has been reported
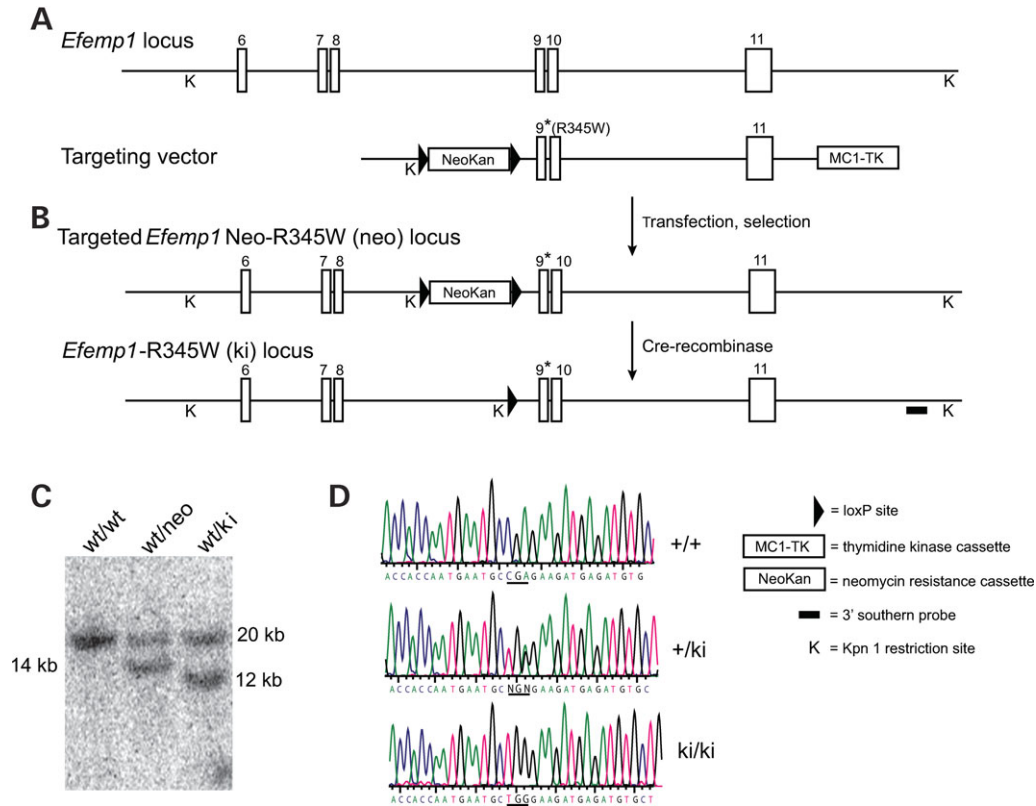
Figure 3. *Efemp1* gene targeting. (**A**) The 3′ end of the mouse *Efemp1* locus and the gene-targeting vector with the R345W mutation are depicted, with numbered exons. (**B**) The targeted *Efemp1* loci are shown. (**C**) Southern blot performed with the indicated 3′ probe showing correct targeting of the *Efemp1* locus in heterozygous wt/neo and wt/ki mice; lane 1 is control wt/wt DNA. The appearance of the 13.8 kb band in the wt/neo sample indicates correct targeting of the *Efemp1* gene. The change in size of the band from the mutant allele to 12 kb indicates successful removal of the floxed neomycin selection cassette in the ki allele. (**D**) Sequence traces from mice of the indicated genotypes following *in vivo* removal of the neomycin cassette. The wild-type codon is CGA, and the mutant (W) codon is TGG. Heterozygous mice show both alleles.

to interact with TIMP3, we also evaluated the location of Timp3 in the retinas of *Efemp1*$^{R345W/R345W}$ mice (31). As shown in Figure 8, the Timp3 signal in Bruch's membrane of the *Efemp1*$^{R345W/R345W}$ mice was thicker than that observed in littermate controls, suggesting that the basal deposits also contain Timp3 protein.

Complement activation and unfolded protein response in *Efemp1*-R345W mice

To assess the status of the complement system in the eyes of *Efemp1*-R345W mice, we stained frozen sections of eyes from 12-month-old wild-type and homozygous *Efemp1*$^{R345W/R345W}$ mice with antibodies to activated complement component C3 (37). C3 is located at the nexus of all three complement activation systems and is thus a good indicator of complement activity (38,39). Activated C3 was detected in the RPE and Bruch's membrane of sections from *Efemp1*$^{R345W/R345W}$ mice. In contrast, no C3 signal was detected in retinas from control mice (Fig. 8).

Prior studies have suggested that mutant Efemp1 protein does not fold properly and is not efficiently secreted from cultured cells (40). The mutant protein has been reported to stimulate an unfolded protein response (UPR) when expressed in ARPE-19 cells (40). To test for the UPR response, we measured the levels of Grp78 in the eyes of wild-type and *Efemp1*-R345W mice by western blotting and evaluated the expression pattern of Grp78 in the retina by immunofluorescence microscopy to localize the protein. No appreciable difference in Grp78 levels was detected and there was no difference in the staining patterns between the mice of different genotypes (Fig. 9).

DISCUSSION

We have evaluated the pathogenicity of the R345W mutation in *EFEMP1* in humans and mice. Our results confirm that this mutation in *EFEMP1* causes the inherited macular degeneration DHRD/ML, as family B has a novel haplotype. In addition, *Efemp1*-R345W knockin mice develop deposits between Bruch's membrane and the RPE, which share several features with basal deposits. The *Efemp1*-R345W knockin mice also demonstrate evidence of alterations in RPE cell ultrastructure, with extensive vacuolization and loss of basolateral infoldings. The basal deposits and altered RPE cell structure in the mutant mice are associated with increased levels of activated complement C3 in Bruch's membrane and the RPE. This finding suggests a connection

A

wt/wt wt/ki ki/ki

2.2kb ———— Efemp1

28S

18S

B

55kDa ———— Efemp1

———— Actin
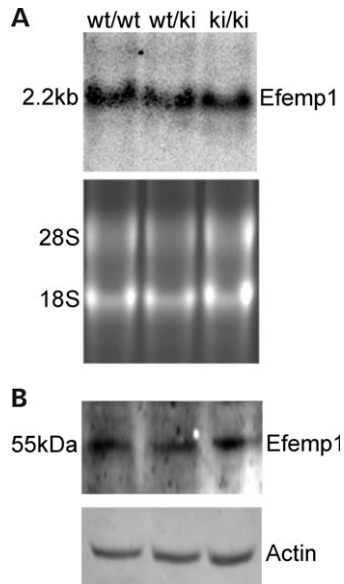
Figure 4. Efemp1 expression in *Efemp1*-R345W mice. (**A**) Top: northern blot of *Efemp1* mRNA expression in retinas of 12-month-old mice of the genotypes indicated. Bottom: image of ethidium bromide-stained agarose gel used for northern blot above demonstrating that equal amounts of RNA were loaded on the gel. (**B**) Top: western blot of retinal protein from 12-month-old mice of the genotypes indicated stained with antibodies to Efemp1. Bottom: the same blot was also probed with antibodies to actin as a loading control.

between alterations in ECM integrity and complement activation.

In the original publication describing the R345W mutation in EFEMP1, all 39 families with this mutation were reported to share common haplotype (9). The complete sharing of alleles of four intragenic *EFEMP1* polymorphisms in these 39 families suggested that the R345W mutation occurred once in a common ancestor, but also raised the possibility that the R345W variant was in linkage disequilibrium with the true disease-causing gene/mutation located nearby. The discovery of a novel, independent haplotype in a family from India with the R345W mutation and DHRD/ML supports the hypothesis that this mutation in *EFEMP1* is indeed the cause of the disease. The finding of more severe phenotypes in the children in family B who are homozygous for the R345W mutation is also consistent with the pathogenicity of this mutation (Fig. 1).

A major finding of our work is that *Efemp1*-R345W knockin mice recapitulate important aspects of the human DHRH/ML phenotype and develop notable deposits between Bruch's and the RPE (Fig. 6). These deposits share several features with basal deposits in patients with early AMD. Specifically, the deposits resemble basal laminar deposits in that they comprised amorphous material with similar electron density to the RPE basal lamina (5). The detection of lesions with wide-spaced collagen in the younger homozygous *Efemp1*$^{R345W/R345W}$ mice suggests that the basal deposits observed may originate in Bruch's membrane.

Immunofluorescence analyses showed that Bruch's membrane in the *Efemp1*$^{R345W/R345W}$ mice contains more Efemp1

and Timp3 than controls (Figs 7 and 8). This suggests that the basal deposits in the mutant mice contain Timp3 and mutant Efemp1, consistent with observations reported for patients with DHRD/ML (30). These findings also suggest that the mutant Efemp1 protein may alter the composition or remodeling of the ECM in Bruch's membrane, leading to basal deposit formation. Additional studies will be required to determine what other proteins are present in the observed basal deposits.

To facilitate the study of AMD, several mouse models of macular degeneration have been recently developed. Some of these display multiple features of AMD, including photo-receptor atrophy and CNV (41–43). Others show more limited features of macular degeneration, including basal deposits in APO B100 transgenic mice, and of basal deposits in *ApoE* knockout and APO*E3-Leiden transgenic mice (44–46). The *Efemp1*-R345W mice are a valuable addition to this group of animal models because of the broad distribution of the basal deposits in the retina and the evidence that the complement system is activated in response to the deposits. The phenotype in the *Efemp1*-R345W mice is also caused by a mutation known to cause human disease, which is not true of the other reported mouse models.

It is not clear how the R345W mutation in EFEMP1 leads to the observed basal deposits. The R345W mutation alters one of the six EGF-like domains in EFEMP1. These calcium binding domains are a common motif among proteins found in the ECM and are thought to facilitate formation of rigid, rod-like structures that are stabilized by interdomain calcium binding and hydrophobic interactions (23,47). The R345W mutation could cause disease by affecting calcium-mediated protein–protein interactions or altering protein structure. In contrast to prior cell culture studies, however, we did not detect an obvious defect in the secretion of the mutant Efemp1 protein *in vivo*, as the mutant protein did not accumulate within RPE cells in the mutant mice (Fig. 7) (30). Further, there was no evidence of an increased UPR on the retinas of the homozygous *Efemp1*$^{R345W/R345W}$ mice (Fig. 9) (40). These differences may be due to the normal levels of expression of the mutant protein in the knockin mice, compared with possible over-expression in transfected cells.

The RPE cells of the *Efemp1*-R345W mutant mice also display alterations, including extensive vacuolization and loss of basolateral infoldings. Although vacuoles have been reported in the RPE cells of older wild-type rodents and were detected in the control mice in our studies, they were much more extensive in the heterozygous and homozygous *Efemp1*-R345W mutant mice (Fig. 6, Table 1) (48). RPE vacuoles have been reported in association with basal deposits in human eyes with AMD (5). Disorganization and disruption of the basal infoldings of the RPE, as seen in the homozygous *Efemp1*$^{R345W/R345W}$ mice, have been observed in samples from patients with basal deposits and early AMD (5).

The basal deposits and RPE alterations in the homozygous *Efemp1*$^{R345W/R345W}$ mice were associated with increased levels of complement C3 activation in Bruch's membrane and the RPE (Fig. 8). As C3 conversion is the end result of all three complement activation pathways, this finding indicates general complement activation (38,39). This finding provides insight into the proposed role of the complement system
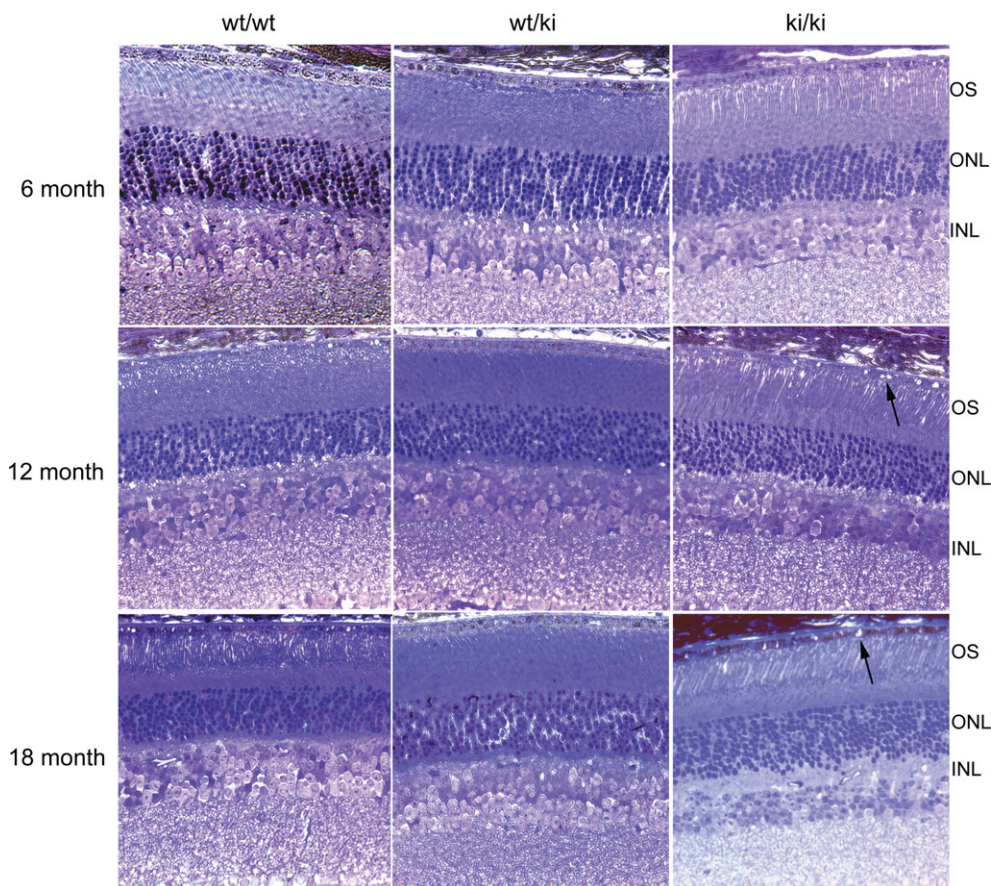
Figure 5. Histology of *Efemp1*-R345W retinas. Retinal sections from mice of the genotypes and ages indicated were stained with Toluidine blue and examined by light microscopy. No changes in retinal health or structure were noted in the mutant mice. Vacuoles were noted in the RPE of homozygous mutant mice starting at 1 year of age (arrows). INL, inner nuclear layer; ONL, outer nuclear layer; OS, outer segment. Magnification 400× for all panels.

in the pathogenesis of AMD. It has been suggested that complement activation in response to the deposition of material in the sub-RPE space plays a role in drusen formation and the development of AMD (20,49). The specific activators of the complement system in this model, however, have not been defined. The result described here suggests that Efemp1 or other ECM components, altered by mutations or aging processes, could be one of the complement activators in the development of AMD. The reported associations between sequence alterations in fibulin-5 in patients with AMD are also consistent with such a model (24). The *Efemp1*-R345W mice provide a useful model for further studies of this hypothesis and the role of ECM proteins in the pathogenesis of macular degeneration.

MATERIALS AND METHODS

Patients

This project was approved by the University of Utah Health Sciences Center Institutional Review Board and informed consent was obtained from all participants in accordance with HIPAA regulations. All subjects underwent ophthalmoscopy and venupuncture. Visual acuity was assessed with a standard Snellen chart. Seventeen members of family A were examined: 10 affected and 7 unaffected. Four affected members of family B were examined, two of whom were homozygous for the R345W mutation.

Genetic analyses

Genomic DNA was extracted from blood samples and genotyping analysis was performed using polymorphic DNA markers encompassing the *EFEMP1* gene. Employed microsatellite markers included D2S378, D2S2352 and intragenic SNPs rs1346786, rs3791676 and rs1430197. For sequencing and genotyping, samples were amplified by the polymerase chain reaction (PCR) and loaded on an ABI 3100 Genetic Analyzer System using established methods (7,50). Direct sequencing was performed with the BigDye Kit (Applied Biosystems, Foster City, CA, USA) according to manufacturer's instructions.

Animals

This research was approved by the University of Pennsylvania for Institutional Animal Care and Use Committee. Wild-type C57BL/6J mice were obtained from Jackson Laboratories or bred from commercially obtained founders.
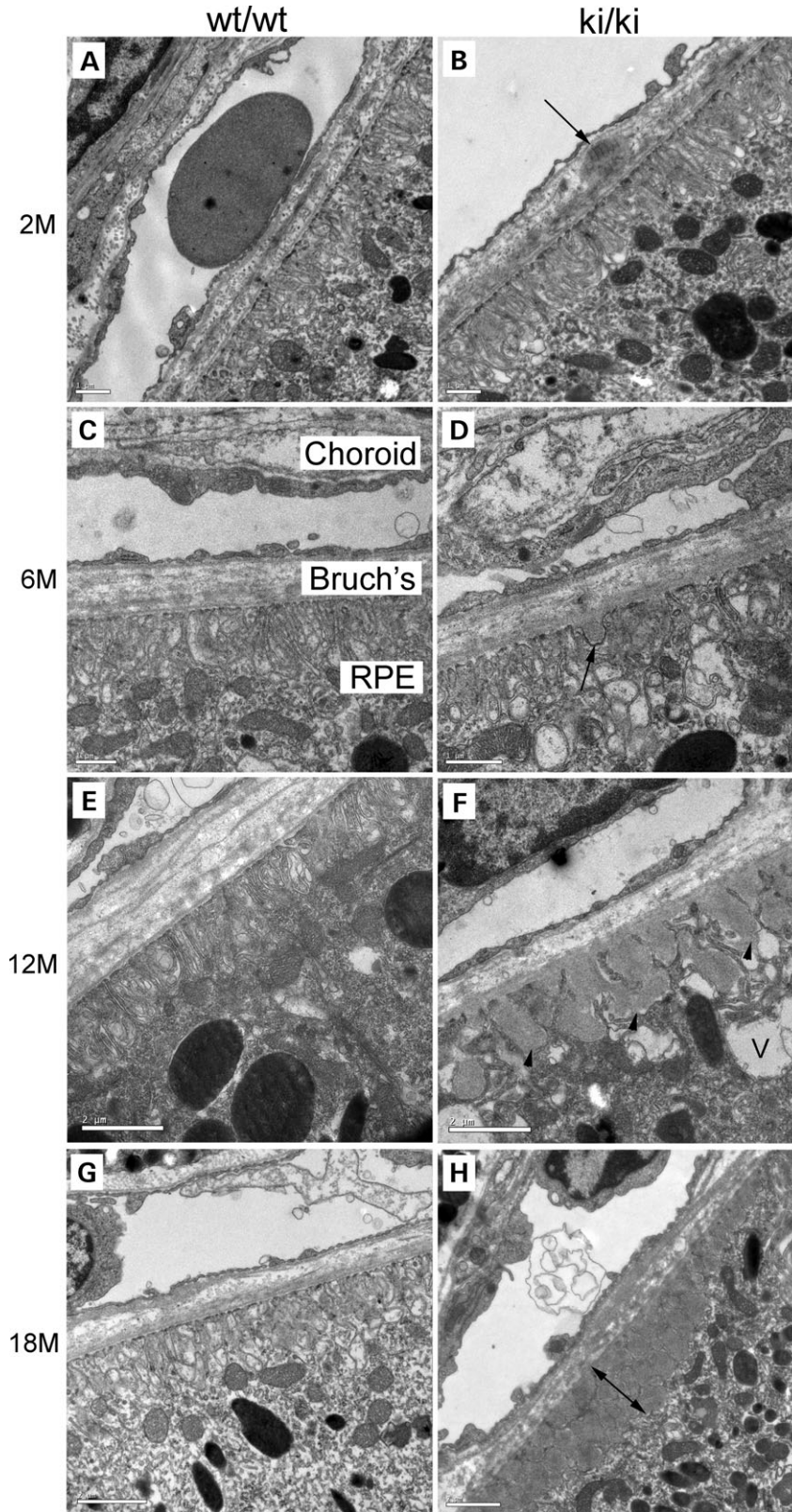
Figure 6. Basal deposits and RPE vacuoles in *Efemp1*-R345W mice. Electron micrographs of the RPE, Bruch's membrane and choroid of wild-type and homozygous knockin (ki/ki) mice at the ages indicated. These layers are labeled in (**C**). At 2 months of age, deposits of wide-spaced collagen were detected in Bruch's membrane of the mutant mice (**B**, arrow). By 6 months of age, small deposits between Bruch's membrane and the RPE were noted (**D**, arrow). At 12 months, extensive deposits were present between Bruch's membrane and the RPE (**F**, arrowheads). Multiple vacuoles were also present in the RPE at this age (V). The deposits were increased in size at 18 months (**H**, arrow). Scale bars = 1 μm for 2- and 6-month images and 2 μm for 12- and 18-month images.

Table 1. Distribution of basal deposits and RPE vacuoles

|	Two months			Six months			Twelve months		
	wt/wt	wt/ki	ki/ki	wt/wt	wt/ki	ki/ki	wt/wt	wt/ki	ki/ki
RPE vacuoles	0/20	0/20	3/20	0/20	3/20	13/20	5/20	11/20	16/20
Basal deposits	0/20	0/20	0/20	0/20	0/20	2/30	0/20	0/20	19/20
Both	0/20	0/20	0/20	0/20	0/20	2/20	0/20	0/20	16/20

Nerve to ora retinal sections were divided into 20 segments, and each segment was scored for the presence of basal deposits and RPE vacuoles using electron microscopy.
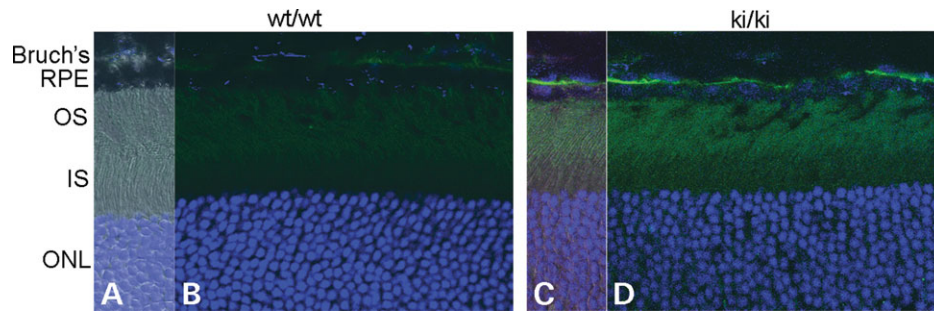
Figure 7. Immunolocalization of Efemp1 protein in the eyes of *Efemp1*-R345W mice. Frozen sections of eye cups from 1-year-old mice of the genotypes indicated were stained with antibodies to Efemp1 (green). Nuclei were detected with Hoechst 33258 (blue). The sections were viewed with fluorescence microscopy alone (**B** and **D**) or in combination with DIC microscopy (**A** and **C**). An increased signal was detected in Bruch's membrane of the mutant mice (C and D).
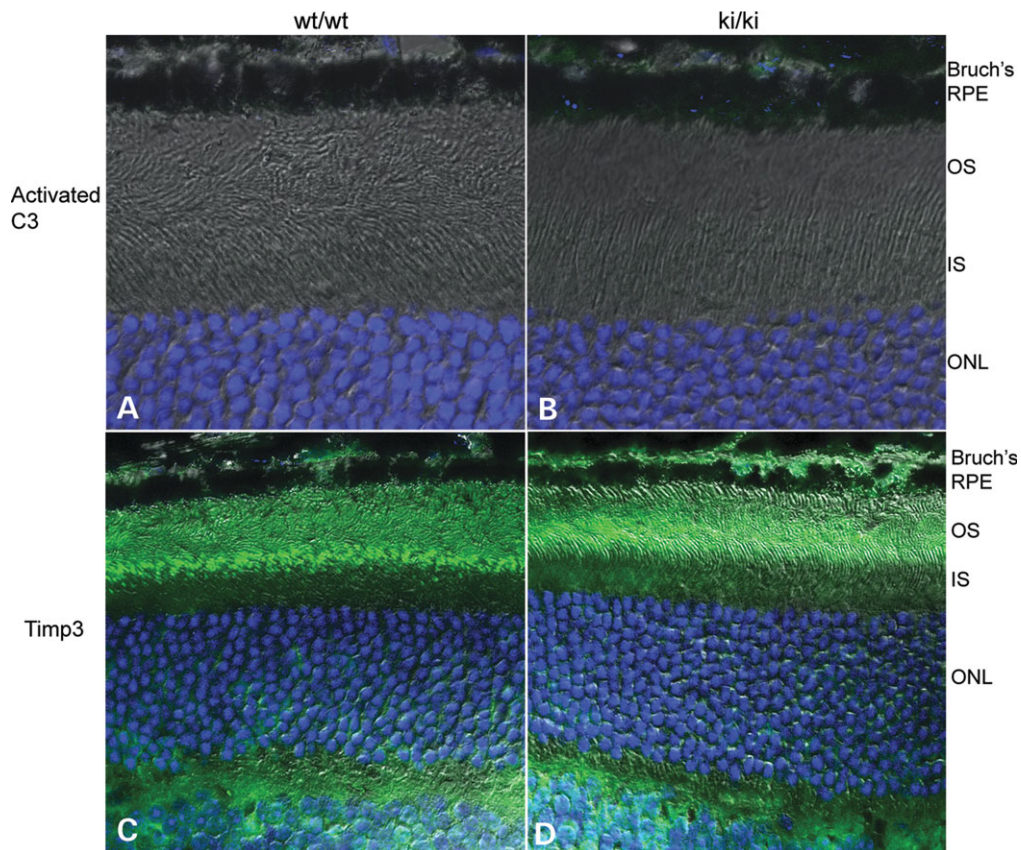
Figure 8. Complement C3 and Timp3 in *Efemp1*-R345W mice. Immunolocalization of activated complement C3 and Timp3 in the eyes of *Efemp1*-R345W mice. Frozen sections of eye cups from 1-year-old mice of the genotypes indicated were stained with antibodies to activated C3 [green (**A**) and (**B**)] or Timp3 [green (**C**) and (**D**)]. Nuclei were detected with Hoechst 33258 (blue). The sections were viewed with fluorescence and DIC microscopy. Increased C3 staining was detected in the RPE and Bruch's membrane of the mutant mice (B). Similarly, increased Timp3 signal was detected in Bruch's membrane of the mutant mice (D).
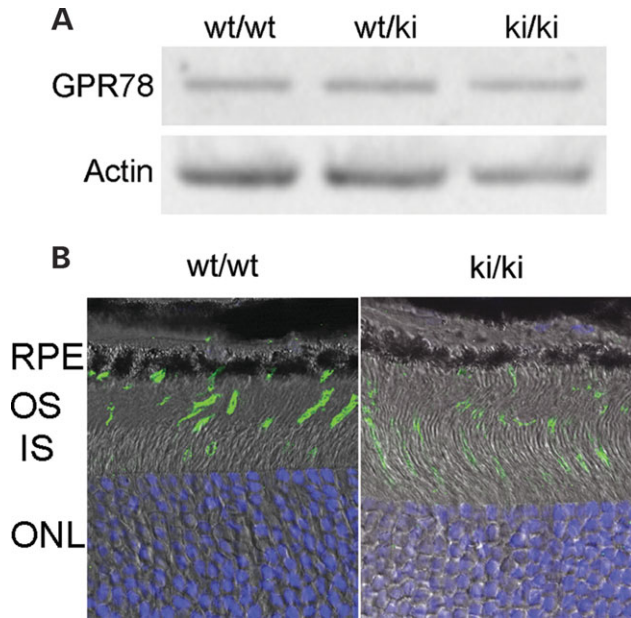
Figure 9. UPR in *Efemp1*-R345W mice. (**A**) Western blot of protein extracts from eyes of 1-year-old mice of the genotypes indicated. The amount of Gpr78 detected was similar for all three genotypes. The same blot was reprobed with antibodies against actin as a loading control. (**B**) Frozen sections of eyes from 1-year-old mice of the genotypes indicated were stained with antibodies to Gpr78 (green). Nuclei were detected with Hoechst 33258 (blue). The sections were viewed with fluorescence and DIC microscopy.

Gene targeting

To create a mouse model of DHRD/ML, we used gene-targeting techniques to introduce the R345W mutation into exon 9, the mouse *Efemp1* gene (Fig. 3). The knockin targeting vector was prepared by isolating a genomic DNA clone from a phage library specifically designed for the production of gene-targeting vectors (33). The R345W mutation (base changes CGA to TGG in codon 345 of the mouse *Efemp1* cDNA, GenBank AK077302) was then introduced into the genomic clone via site-directed mutagenesis. The completed vector was transfected into 129SvEvTac mouse ES cells, and the G418/ganciclovir-resistant colonies screened for the correct recombination by PCR and Southern blotting. Six out of 192 ES cell colonies demonstrated correct targeting (data not shown).

Two different clones of the *Efemp1*-Neo-R345W knockin ES cells were injected into blastocysts, and 11 highly chimeric mice produced. The chimeric founder mice were backcrossed with C57BL/6J and 129SvEvTac mice. Agouti F1 progeny were screened for the targeted *Efemp1*-Neo-R345W allele by PCR and Southern blotting using genomic DNA isolated from tail biopsies. Seven of the 11 chimeras bred to date have passed the mutant allele to their offspring (data not shown). To produce mice with the final *Efemp1*-R345W knockin allele, we crossed F1 *Efemp1*-Neo-R345W mice with *EIIa-Cre* mice to remove the neomycin selection cassette (34). As there can be mosaicism in Cre-mediated excision in some tissues of EIIa-cre progeny, the F1 *Efemp1*-R345W mice were backcrossed with C57BL/6 mice to establish a line of knockin mice with complete excision of the selection cassette and that is Cre-negative (Fig. 1). These N1 C57BL/6 *Efemp1*-R345W mice were bred to produce stocks of heterozygous and homozygous mice.

Immunofluorescence microscopy

Eyes from wild-type and mutant mice were enucleated after cardiac perfusion with 4% paraformaldehyde in phosphate-buffered saline (PBS) (pH 7.4) and fixed in 4% paraformaldehyde for 3 h, embedded in optimal cutting temperature (OCT) freezing media and cryosectioned at 10 μm. The frozen sections were then immunostained, as described previously (51). The primary antibodies used were anti-Efemp1 [a gift from Dr Takako Sasaki, Shriners Hospital for Children, Portland, OR, USA (52)], anti-activated C3 [a gift from Dr John Lambris, University of Pennsylvania School of Medicine (37)], anti-Timp3 (Sigma, St Louis, MO, USA) and anti-Grp78 (N-20, Santa Cruz Biotechnology, Santa Cruz, CA, USA). Cy3, Alexa 468 and Alexa 633 conjugated secondary antibodies were obtained from Jackson ImmunoResearch or Molecular Probes. Stained sections were viewed with a Zeiss LSM 510 Meta confocal microscope and the images processed with Zeiss Meta 510 software (Carl Zeiss MicroImaging).

Histology and ultrastructure

Eye cups from wild-type and mutant mice of the desired age were fixed in 0.05% glutaraldehyde plus 2% paraformaldehyde in PBS, pH 7.4, for 1 h. Tissues were then dehydrated in a graded ethanol series, infiltrated and embedded in EMbed812 (Electron Microscopy Sciences). For histological studies, thick (1–2 μm) sections were cut and stained with Toluidine blue. For ultrastructural analyses, ultrathin sections (70 nm) were cut, stained with lead citrate and uranyl acetate and examined using a Tecnai 12 Twin transmission electron microscope.

Northern, Southern and western blotting

Northern blotting was performed as described using total mouse retinal RNA and an [α-^{32}P]dCTP-labeled cDNA probe, and the blots analyzed on a Storm 860 PhosphorImager (Molecular Dynamics, Sunnyvale, CA, USA) (53). Southern blotting was performed according to established methods using genomic DNA isolated from tail biopsies (32). Western blotting was performed as described, using the antibodies indicated (51). Positive signals were visualized and quantified by fluorimetry using the Storm 860 PhosphorImager.

SUPPLEMENTARY MATERIAL

Supplementary Material is available at HMG Online.

REFERENCES

1. Klein, R., Klein, B.E. and Linton, K.L.P. (1992) Prevalence of age-related maculopathy—the Beaver Dam Eye Study. *Ophthalmology*, **99**, 933–943.
2. Hageman, G.S. and Mullins, R.F. (1999) Molecular composition of drusen as related to substructural phenotype. *Mol. Vis.*, **5**, 28.
3. Lin, R.C. and Rosenfeld, P.J. (2007) Antiangiogenic therapy in neovascular age-related macular degeneration. *Int. Ophthalmol. Clin.*, **47**, 117–137.
4. Age-Related Eye Disease Study Research Group (2001) A randomized, placebo-controlled, clinical trial of high-dose supplementation with vitamins C and E, beta carotene, and zinc for age-related macular degeneration and vision loss: AREDS report no. 8. *Arch. Ophthalmol.*, **119**, 1417–1436.
5. Curcio, C.A. and Millican, C.L. (1999) Basal linear deposit and large drusen are specific for early age-related maculopathy. *Arch. Ophthalmol.*, **117**, 329–339.
6. Allikmets, R., Singh, N., Sun, H., Shroyer, N.F., Hutchinson, A., Chidambaram, A., Gerrard, B., Baird, L., Stauffer, D., Peiffer, A. *et al.* (1997) A photoreceptor cell-specific ATP-binding transporter gene (ABCR) is mutated in recessive Stargardt macular dystrophy. *Nat. Genet.*, **15**, 236–246.
7. Zhang, K., Kniazeva, M., Han, M., Li, W., Yu, Z., Yang, Z., Li, Y., Metzker, M.L., Allikmets, R., Zack, D.J. *et al.* (2001) A 5-bp deletion in ELOVL4 is associated with two related forms of autosomal dominant macular dystrophy. *Nat. Genet.*, **27**, 89–93.
8. Weber, B.H., Vogt, G., Pruett, R.C., Stohr, H. and Felbor, U. (1994) Mutations in the tissue inhibitor of metalloproteinases-3 (TIMP3) in patients with Sorsby's fundus dystrophy. *Nat. Genet.*, **8**, 352–356.
9. Stone, E.M., Lotery, A.J., Munier, F.L., Heon, E., Piguet, B., Guymer, R.H., Vandenburgh, K., Cousin, P., Nishimura, D., Swiderski, R.E. *et al.* (1999) A single EFEMP1 mutation associated with both Malattia Leventinese and Doyne honeycomb retinal dystrophy. *Nat. Genet.*, **22**, 199–202.
10. Hayward, C., Shu, X., Cideciyan, A.V., Lennon, A., Barran, P., Zareparsi, S., Sawyer, L., Hendry, G., Dhillon, B., Milam, A.H. *et al.* (2003) Mutation in a short-chain collagen gene, CTRP5, results in extracellular deposit formation in late-onset retinal degeneration: a genetic model for age-related macular degeneration. *Hum. Mol. Genet.*, **12**, 2657–2667.
11. Klein, R.J., Zeiss, C., Chew, E.Y., Tsai, J.Y., Sackler, R.S., Haynes, C., Henning, A.K., SanGiovanni, J.P., Mane, S.M., Mayne, S.T. *et al.* (2005) Complement factor H polymorphism in age-related macular degeneration. *Science*, **308**, 385–389.
12. Edwards, A.O., Ritter, R., III, Abel, K.J., Manning, A., Panhuysen, C. and Farrer, L.A. (2005) Complement factor H polymorphism and age-related macular degeneration. *Science*, **308**, 421–424.
13. Haines, J.L., Hauser, M.A., Schmidt, S., Scott, W.K., Olson, L.M., Gallins, P., Spencer, K.L., Kwan, S.Y., Noureddine, M., Gilbert, J.R. *et al.* (2005) Complement factor H variant increases the risk of age-related macular degeneration. *Science*, **308**, 419–421.
14. Hageman, G.S., Anderson, D.H., Johnson, L.V., Hancox, L.S., Taiber, A.J., Hardisty, L.I., Hageman, J.L., Stockman, H.A., Borchardt, J.D., Gehrs, K.M. *et al.* (2005) A common haplotype in the complement regulatory gene factor H (HF1/CFH) predisposes individuals to age-related macular degeneration. *Proc. Natl Acad. Sci. USA*, **102**, 7227–7232.
15. Conley, Y.P., Thalamuthu, A., Jakobsdottir, J., Weeks, D.E., Mah, T., Ferrell, R.E. and Gorin, M.B. (2005) Candidate gene analysis suggests a role for fatty acid biosynthesis and regulation of the complement system in the etiology of age-related maculopathy. *Hum. Mol. Genet.*, **14**, 1991–2002.
16. Zareparsi, S., Branham, K.E., Li, M., Shah, S., Klein, R.J., Ott, J., Hoh, J., Abecasis, G.R. and Swaroop, A. (2005) Strong association of the Y402H variant in complement factor H at 1q32 with susceptibility to age-related macular degeneration. *Am. J. Hum. Genet.*, **77**, 149–153.
17. Zareparsi, S., Buraczynska, M., Branham, K.E., Shah, S., Eng, D., Li, M., Pawar, H., Yashar, B.M., Moroi, S.E., Lichter, P.R. *et al.* (2005) Toll-like receptor 4 variant D299G is associated with susceptibility to age-related macular degeneration. *Hum. Mol. Genet.*, **14**, 1449–1455.
18. Yang, Z., Camp, N.J., Sun, H., Tong, Z., Gibbs, D., Cameron, D.J., Chen, H., Zhao, Y., Pearson, E., Li, X. *et al.* (2006) A variant of the HTRA1 gene increases susceptibility to age-related macular degeneration. *Science*, **314**, 992–993.
19. Dewan, A., Liu, M., Hartman, S., Zhang, S.S., Liu, D.T., Zhao, C., Tam, P.O., Chan, W.M., Lam, D.S., Snyder, M. *et al.* (2006) HTRA1 promoter polymorphism in wet age-related macular degeneration. *Science*, **314**, 989–992.
20. Anderson, D.H., Mullins, R.F., Hageman, G.S. and Johnson, L.V. (2002) A role for local inflammation in the formation of drusen in the aging eye. *Am. J. Ophthalmol.*, **134**, 411–431.
21. Dunaief, J.L. (2006) Iron induced oxidative damage as a potential factor in age-related macular degeneration: the Cogan Lecture. *Invest. Ophthalmol. Vis. Sci.*, **47**, 4660–4664.
22. Grau, S., Richards, P.J., Kerr, B., Hughes, C., Caterson, B., Williams, A.S., Junker, U., Jones, S.A., Clausen, T. and Ehrmann, M. (2006) The role of human HtrA1 in arthritic disease. *J. Biol. Chem.*, **281**, 6124–6129.
23. Timpl, R., Sasaki, T., Kostka, G. and Chu, M.L. (2003) Fibulins: a versatile family of extracellular matrix proteins. *Nat. Rev. Mol. Cell Biol.*, **4**, 479–489.
24. Stone, E.M., Braun, T.A., Russell, S.R., Kuehn, M.H., Lotery, A.J., Moore, P.A., Eastman, C.G., Casavant, T.L. and Sheffield, V.C. (2004) Missense variations in the fibulin 5 gene and age-related macular degeneration. *N. Engl. J. Med.*, **351**, 346–353.
25. Loeys, B., Van Maldergem, L., Mortier, G., Coucke, P., Gerniers, S., Naeyaert, J.M. and De Paepe, A. (2002) Homozygosity for a missense mutation in fibulin-5 (FBLN5) results in a severe form of cutis laxa. *Hum. Mol. Genet.*, **11**, 2113–2118.
26. Yanagisawa, H., Davis, E.C., Starcher, B.C., Ouchi, T., Yanagisawa, M., Richardson, J.A. and Olson, E.N. (2002) Fibulin-5 is an elastin-binding protein essential for elastic fibre development *in vivo*. *Nature*, **415**, 168–171.
27. McLaughlin, P.J., Chen, Q., Horiguchi, M., Starcher, B.C., Stanton, J.B., Broekelmann, T.J., Marmorstein, A.D., McKay, B., Mecham, R., Nakamura, T. and Marmorstein, L.Y. (2006) Targeted disruption of fibulin-4 abolishes elastogenesis and causes perinatal lethality in mice. *Mol. Cell Biol.*, **26**, 1700–1709.
28. Hucthagowder, V., Sausgruber, N., Kim, K.H., Angle, B., Marmorstein, L.Y. and Urban, Z. (2006) Fibulin-4: a novel gene for an autosomal recessive cutis laxa syndrome. *Am. J. Hum. Genet.*, **78**, 1075–1080.
29. Blackburn, J., Tarttelin, E.E., Gregory-Evans, C.Y., Moosajee, M. and Gregory-Evans, K. (2003) Transcriptional regulation and expression of the dominant drusen gene FBLN3 (EFEMP1) in mammalian retina. *Invest. Ophthalmol. Vis. Sci.*, **44**, 4613–4621.
30. Marmorstein, L.Y., Munier, F.L., Arsenijevic, Y., Schorderet, D.F., McLaughlin, P.J., Chung, D., Traboulsi, E. and Marmorstein, A.D. (2002) Aberrant accumulation of EFEMP1 underlies drusen formation in Malattia Leventinese and age-related macular degeneration. *Proc. Natl Acad. Sci. USA*, **99**, 13067–13072.
31. Klenotic, P.A., Munier, F.L., Marmorstein, L.Y. and nand-Apte, B. (2004) Tissue inhibitor of metalloproteinases-3 (TIMP-3) is a binding partner of epithelial growth factor-containing fibulin-like extracellular matrix protein 1 (EFEMP1). Implications for macular degenerations. *J. Biol. Chem.*, **279**, 30469–30473.
32. Nagy, A., Gertsenstein, M., Vintersten, K. and Behringer, R.R. (2003) *Manipulating the Mouse Embyro*, Woodbury, NY, USA.
33. Zhang, P., Li, M.Z. and Elledge, S.J. (2002) Towards genetic genome projects: genomic library screening and gene-targeting vector construction in a single step. *Nat. Genet.*, **30**, 31–39.
34. Lakso, M., Pichel, J.G., Gorman, J.R., Sauer, B., Okamoto, Y., Lee, E., Alt, F.W. and Westphal, H. (1996) Efficient *in vivo* manipulation of mouse genomic sequences at the zygote stage. *Proc. Natl Acad. Sci. USA*, **93**, 5860–5865.

35. Mishima, H. and Hasebe, H. (1978) Some observations in the fine structure of age changes of the mouse retinal pigment epithelium. *Albrecht. Von. Graefes Arch. Klin. Exp. Ophthalmol.*, **209**, 1–9.

36. Fan, W., Lin, N., Sheedlo, H.J. and Turner, J.E. (1996) Muller and RPE cell response to photoreceptor cell degeneration in aging Fischer rats. *Exp. Eye Res.*, **63**, 9–18.

37. Mastellos, D., Prechl, J., Laszlo, G., Papp, K., Olah, E., Argyropoulos, E., Franchini, S., Tudoran, R., Markiewski, M., Lambris, J.D. and Erdei, A. (2004) Novel monoclonal antibodies against mouse C3 interfering with complement activation: description of fine specificity and applications to various immunoassays. *Mol. Immunol.*, **40**, 1213–1221.

38. Walport, M.J. (2001) Complement. Second of two parts. *N. Engl. J. Med.*, **344**, 1140–1144.

39. Walport, M.J. (2001) Complement. First of two parts. *N. Engl. J. Med.*, **344**, 1058–1066.

40. Roybal, C.N., Marmorstein, L.Y., Vander Jagt, D.L. and Abcouwer, S.F. (2005) Aberrant accumulation of fibulin-3 in the endoplasmic reticulum leads to activation of the unfolded protein response and VEGF expression. *Invest. Ophthalmol. Vis. Sci.*, **46**, 3973–3979.

41. Ambati, J., Anand, A., Fernandez, S., Sakurai, E., Lynn, B.C., Kuziel, W.A., Rollins, B.J. and Ambati, B.K. (2003) An animal model of age-related macular degeneration in senescent Ccl-2- or Ccr-2-deficient mice. *Nat. Med.*, **9**, 1390–1397.

42. Hahn, P., Qian, Y., Dentchev, T., Chen, L., Beard, J., Harris, Z.L. and Dunaief, J.L. (2004) Disruption of ceruloplasmin and hephaestin in mice causes retinal iron overload and retinal degeneration with features of age-related macular degeneration. *Proc. Natl Acad. Sci. USA*, **101**, 13850–13855.

43. Karan, G., Lillo, C., Yang, Z., Cameron, D.J., Locke, K.G., Zhao, Y., Thirumalaichary, S., Li, C., Birch, D.G., Vollmer-Snarr, H.R. *et al.* (2005) Lipofuscin accumulation, abnormal electrophysiology, and photoreceptor degeneration in mutant ELOVL4 transgenic mice: a model for macular degeneration. *Proc. Natl Acad. Sci. USA*, **102**, 4164–4169.

44. Kliffen, M., Lutgens, E., Daemen, M.J., de Muinck, E.D., Mooy, C.M. and de Jong, P.T. (2000) The APO(*)E3-Leiden mouse as an animal model for basal laminar deposit. *Br. J. Ophthalmol.*, **84**, 1415–1419.

45. Dithmar, S., Curcio, C.A., Le, N.A., Brown, S. and Grossniklaus, H.E. (2000) Ultrastructural changes in Bruch's membrane of apolipoprotein E-deficient mice. *Invest. Ophthalmol. Vis. Sci.*, **41**, 2035–2042.

46. Espinosa-Heidmann, D.G., Sall, J., Hernandez, E.P. and Cousins, S.W. (2004) Basal laminar deposit formation in APO B100 transgenic mice: complex interactions between dietary fat, blue light, and vitamin E. *Invest Ophthalmol. Vis. Sci.*, **45**, 260–266.

47. Downing, A.K., Knott, V., Werner, J.M., Cardy, C.M., Campbell, I.D. and Handford, P.A. (1996) Solution structure of a pair of calcium-binding epidermal growth factor-like domains: implications for the Marfan syndrome and other genetic disorders. *Cell*, **85**, 597–605.

48. Lin, N., Fan, W., Sheedlo, H.J. and Turner, J.E. (1997) Basic fibroblast growth factor treatment delays age-related photoreceptor degeneration in Fischer 344 rats. *Exp. Eye Res.*, **64**, 239–248.

49. Hageman, G.S., Luthert, P.J., Victor Chong, N.H., Johnson, L.V., Anderson, D.H. and Mullins, R.F. (2001) An integrated hypothesis that considers drusen as biomarkers of immune-mediated processes at the RPE-Bruch's membrane interface in aging and age-related macular degeneration. *Prog. Retin. Eye Res.*, **20**, 705–732.

50. Yang, Z., Peachey, N.S., Moshfeghi, D.M., Thirumalaichary, S., Chorich, L., Shugart, Y.Y., Fan, K. and Zhang, K. (2002) Mutations in the RPGR gene cause X-linked cone dystrophy. *Hum. Mol. Genet.*, **11**, 605–611.

51. Liu, Q., Zhou, J., Daiger, S.P., Farber, D.B., Heckenlively, J.R., Smith, J.E., Sullivan, L.S., Zuo, J., Milam, A.H. and Pierce, E.A. (2002) Identification and subcellular localization of the RP1 protein in human and mouse photoreceptors. *Invest. Ophthalmol. Vis. Sci.*, **43**, 22–32.

52. Kobayashi, N., Kostka, G., Garbe, J.H., Keene, D.R., Bachinger, H.P., Hanisch, F.G., Markova, D., Tsuda, T., Timpl, R., Chu, M.L. and Sasaki, T. (2007) A comparative analysis of the fibulin protein family: biochemical characterization, binding interactions and tissue localization. *J. Biol. Chem.*, **282**, 11805–11816.

53. Pierce, E.A., Quinn, T., Meehan, T., McGee, T.L., Berson, E.L. and Dryja, T.P. (1999) Mutations in a gene encoding a new oxygen-regulated photoreceptor protein cause dominant retinitis pigmentosa. *Nat. Genet.*, **22**, 248–254.